Biaxial ordering, self-diffusion, and helix-distortion effects on ^{2}H NMR spectral patterns from cholesteric liquid crystals

Giuseppe Chidichimo,* Zvi Yaniv, Nuno A. P. Vaz,† and J. William Doane
Department of Phsyics and Liquid Crystal Institute, Kent State University, Kent, Ohio 44242
(Received 7 August 1981)

Deuterium NMR spectral patterns from cholesteric liquid crystals (twisted nematics) for the case where the pitch axis aligns perpendicular to the direction of the magnetic field are evaluated in terms of three quantities or effects: (i) an asymmetry parameter in the quadrupole interaction which has been motionally induced by biaxial ordering of the molecules, (ii) a self-diffusion constant for migration of the molecules along the pitch axis, and (iii) distortion of the cholesteric helix in the presence of the applied magnetic field. Calculated spectral patterns which include the above effects are fitted to experimentally recorded spectral patterns from a selectively deuterated nematic that has been twisted by the addition of a chiral compound. It is demonstrated how values of the asymmetry parameter and the self-diffusion constant can be separately measured and helix-distortion-effects studied.

I. INTRODUCTION

Nuclear magnetic resonance (NMR) spectral ("powder") patterns from cholesteric liquid crystals provide a wealth of information regarding microscopic and macroscopic features of this particular phase. The shape of the patterns are sensitive to different aspects of the molecular orientational order,[1-4] to self-diffusion along the pitch axis,[1-5] and to the details of the manner in which the helix becomes distorted and untwisted by the applied magnetic field or other interactions.[6-8]

The spectral patterns result in that the twisted nematic structure consists of a distribution of directors relative to the direction of the applied magnetic field, $\vec{H}$. There are three cases which often arise in practice, depending upon the anisotropy of the diamagnetic susceptibility of the sample: (i) The pitch axis is aligned by the magnetic field in a direction parallel to $\vec{H}$, in which case the directors are all perpendicular to $\vec{H}$ and there is no distribution at all to create a spectral pattern other than that of the characteristic spectra of an aligned sample. This case often happens when derivatives of cholesterol are used[3] and is not a desirable case to have when studying or identifying some aspects of orientational order, self-diffusion, or when examining the structure of the helical twist; (ii) The pitch axis is aligned perpendicular to the direction of $\vec{H}$, imposing a cylindrical distribution of directors. This is the case to be studied here and is the case best suited for most accurately obtaining measurements of the molecular-order parameters and self-diffusion constant as well as obtaining details on the helical structure; (iii) A third case has been reported to occur[1] where the magnetic field does not align the pitch axes at all and there is an isotropic distribution of directors. In this case, the same features of the cholesteric phase can be studied as in the second case above, except with less sensitivity, accuracy, and simplicity.

Recently, we reported on some studies of deuterium spectral patterns from a selectively deuterated nematic that was twisted about a direction perpendicular to $\vec{H}$ by the addition of a chiral compound.[4,5] Because of the suitability of this configuration for precise measurements, we were able to report on some features of the cholesteric phase never observed or measured before. These data indicated that the molecules were biaxially ordered;[4] a feature predicted several years ago by theoretical investigations[9-11] but never before confirmed experimentally. The data also indicated that the self-diffusion constant along the pitch axis increases with decreasing pitch,[5] a feature which might have been expected from viscosity studies[12] but never reported in the literature. And finally we found a new variant of modulated diffusion which occurs when the helix is distorted by the magnetic field.[13]

In this paper we provide details that were not provided in previous publications on the effects of biaxial ordering, self-diffusion, and helical structure on the overall shape of the spectral patterns. We show how each of these effects or quantities

can be studied or measured separately. Fits to experimental data are shown to illustrate the features of the theory and the accuracy of the measurements.

II. CALCULATION OF THE SPECTRAL PATTERNS

The Larmor frequency of the quadrupole interaction for deuterium (spin $I=1$) is obtained experimentally in terms of the splitting between a two-line spectrum, which can be expressed as[14]

$$\omega(\theta_0)=\pm\tfrac{3}{16}\nu_Q[(1+\eta\cos2\phi)+(3-\eta\cos2\phi)\cos2\theta], \quad (1)$$

where θ and ϕ are the polar and azimuthal angles giving the direction of the magnetic field in the principal axis system. The other symbols are the time-averaged quadrupole-coupling constant, $\nu_Q=eQV_{zz}/h$, and the asymmetry parameter, $\eta=(V_{xx}-V_{yy})/V_{zz}$. The coordinates x,y,z are the principal axes associated with the liquid-crystalline phase and V_{ii} are the components of the electric field gradient tensor that result following the time-averaging processes in the liquid crystal. In the liquid-crystal phase a motionally induced asymmetry parameter is a signature for biaxial ordering.[4,15] When the nematic is untwisted, it is uniaxial, and z aligns parallel to $\vec{H}$. When the nematic becomes twisted by the chiral compound, the pitch axis is an axis of symmetry, and defines either the x or the y principal axis. By convention,[14] x is defined such that $|V_{xx}|$ is the smallest component of the electric field gradient. In the compounds studied to date[4] it is found that x is the pitch axis under this convention.

In the cholesteric phase where the pitch axis is perpendicular to the direction of the magnetic field, Eq. (1) becomes further time averaged by translational diffusion along the pitch axis. Brownian translation of the molecules along the pitch axis during the time scale of the measurement corresponds to an effective reorientation of the molecular long axis, i.e., a translational jump requires a rotational jump. With this simple model the time-averaging process can be described in a straightforward manner. We regard a molecule to be situated at an arbitrary position x_0 on the pitch axis at a time $t=0$. If the diffusion process is Markovian, then at a time t the probability that the Brownian motion brings the molecule to a new position x on the pitch axis can be described by the Gaussian function[16]

$$P(x_0x,t)=\frac{1}{\sqrt{2\pi}\sqrt{2Dt}}\exp\left[\frac{(x-x_0)^2}{4Dt}\right], \quad (2)$$

where D is the self-diffusion constant along the pitch axis. In the application of Eq. (2) we consider two cases: case A, where the cholesteric helix is undistorted by the magnetic field; and case B where it is distorted.

A. Undistorted helical structure

In this case there is a linear relationship between x and θ which allows one to write

$$(x-x_0)=\frac{p_0}{2\pi}(\theta-\theta_0), \quad (3)$$

where p_0 is the pitch length. For a discrete time t Eq. (1) becomes averaged according to the relation

$$\bar{\omega}(\theta_0,t)=\int_{-\infty}^{\infty}P(\theta_0,\theta,t)\omega(\theta)\,d\theta=\pm\tfrac{3}{16}\nu_Q\left[(1-\eta)+(3+\eta)\cos2\theta_0\exp\left[\frac{-16\pi^2Dt}{p_0^2}\right]\right], \quad (4)$$

where the constraint $\phi=\pi/2$ is imposed by the choice of x as the pitch axis. It is noted that Eq. (4) has the proper limits for $D=0$ and ∞.

The free-induction decay, $G(t)$, or one-half of the quadrupolar echo, can be expressed in terms of the ensemble average[14]

$$G(t)=\left\langle\exp\left[i\int_0^t\omega(t')\,dt'\right]\right\rangle.$$

Maintaining only the real part we write

$$G(t)=G_0\int_0^{\pi/2}\left[\cos\int_0^t\bar{\omega}(\theta_0t')\,dt'\right]\times R(\theta_0,t+2\tau)U(\theta_0)\,d\theta_0, \quad (5)$$

where G_0 is a constant and θ_0 is distributed according to the function $U(\theta_0)$. In the case of the undistorted helix $U(\theta_0)=1$. $R(\theta_0,t+2\tau)$ is a relaxation function which accounts for line broadening due to magnetic dipole-dipole interactions and magnetic field inhomogeneities. The time τ is that associated with the quadrupole echo.[17] The damping function $R(\theta_0,t)$ was taken to be

$$R(\theta_0,t)=\exp[-t^2\sigma^2(\theta_0)/2] ,$$

where

$$\sigma(\theta_0)=W'+W''[\,|P_2(\cos\theta_0)|-1] ,$$

where W' and W'' are fitting parameters.[18] Performing the integration on dt' in Eq. (5) we obtain for the free-induction decay

$$G(t)=G_0\int_0^{\pi/2}\{\cos[\Omega(\theta_0,t)t]\}\times R(\theta_0,t+2\tau)d\theta_0 , \tag{6a}$$

where

$$\Omega(\theta_0,t)=\tfrac{3}{16}\nu_Q[(1-\eta)+(3+\eta)K\cos 2\theta_0] , \tag{6b}$$

and where

$$K=\frac{p_0^2}{16\pi^2Dt}\left[1-\exp\left[\frac{-16\pi^2Dt}{p_0^2}\right]\right] . \tag{6c}$$

The spectral pattern can be obtained by the Fourier transformation of Eq. (6). Figure 1 shows spectral patterns calculated in this manner for different values of the diffusion constant. The spectral pattern reduces to a spectrum of two lines for rapid diffusion as expected and in agreement with Luz *et al.*,[3] who used another numerical technique to calculate the spectral patterns but did not include the possibility of a finite η.

While Eq. (6) can be readily evaluated numerically, there are some useful features and simplifications that are worth noting. If we regard t_m as the length of the free-induction decay, then $\Omega(\theta_0,t_m)$ of Eqs. (6b) can be considered to be the average frequency over the time interval from $t=0$ to $t=t_m$. We shall subsequently show that it is a good approximation to express Eq. (6) as

$$G(t)=G_0\int_0^{\pi/2}\{\cos[\Omega(\theta_0,t_m)t]\}\times R(\theta_0,t+2\tau)d\theta_0 . \tag{7}$$

This approximation allows us to obtain a useful expression for the position of the characteristic singularities which arise in the spectral pattern. Ignoring the line-broadening function and changing the variable of integration in Eq. (7) from θ_0 to

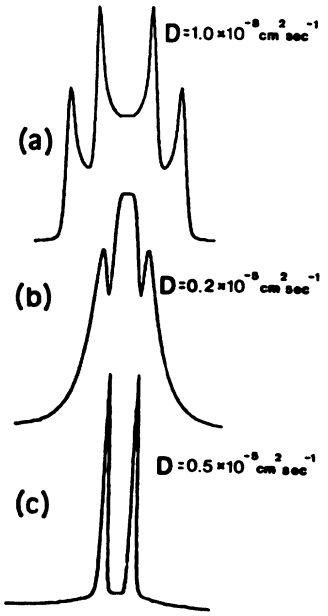

FIG. 1. Calculated spectral patterns from Eq. (6) illustrating the effect of molecular self-diffusion along the pitch axis in a sample where the helix is undistorted by the magnetic field. The spectral patterns were calculated for the values of the diffusion constant D indicated in the figure and for $\eta=0$.

Ω, the Fourier transform of Eq. (7) is trivially calculated yielding the cylindrically distributed spectral pattern which consists of two sets of edge singularities of the type which appeared in other liquid-crystal investigations.[19,20] The splittings $\delta\nu_1$ between the outer-edge singularities and $\delta\nu_2$ between the inner set can be obtained experimentally with high precision. From the Fourier transform of Eq. (7) with $R=1$ they are calculated to be

$$\begin{aligned}\delta\nu_1&=\tfrac{3}{8}\nu_Q[(1-\eta)+(3+\eta)K] ,\\ \delta\nu_2&=\pm\tfrac{3}{8}\nu_Q[(1-\eta)-(3+\eta)K] ,\end{aligned} \tag{8}$$

an expression made use of in our previous studies of the cholesteric phase.[4,5] In the expression for $\delta\nu_2$ the plus sign is to be considered whenever the self-diffusion is sufficiently large to force the singularities that define $\delta\nu_2$ to cross over zero, i.e., $(1-\eta)<(3+\eta)K$. Otherwise, $\delta\nu_2$ is negative. Including the line-broadening term has only the effect of broadening the singularities and Eq. (8) remains valid.

We also find that the values of η measured by using either Eq. (8) or the more exact curve-fitting procedure described by Eqs. (6), are always identi-

cal. This is illustrated in Fig. 2 where we compare experimental spectral patterns with calculated patterns using Eqs. (6) as well as Eq. (7). The experimental patterns were obtained from a nematic material consisting of a binary mixture of 75 wt. % 4-methoxybenzylidene-4'-*n*-butylaniline (MBBA) and 25 wt. % 4-*n*-butyloxybenzylidene-4'-*n*-heptyl-d_4-aniline (40,7-d_4) selectively deuterated in the aromatic ring. To this was added 8 wt. % of chiral 4-cyano-4'-(2-methyl)butylbiphenyl (CB-15) to yield the twisted structure. Figures 2(a) and 2(d) show experimental spectra obtained, respectively, at 291.16 K and 313.96 K. Figures 2(b) and 2(e) show the best fit using Eqs. (6) and Figs. 2(c) and 2(f) show the best fit using Eq. (7). Values of η can be calculated using Eq. (8) and the positions of the singularities from the quantity $\Delta=\delta\nu_1-\delta\nu_2$ as discussed in Ref. 4. As seen from Eq. (8) the quantity Δ is independent of diffusion effects. This can also be seen to be true for the patterns shown in Fig. 1 and also those of Luz *et al.*[3] Equation (8) gives values of $\eta_a=0.06\pm0.01$ and $\eta_d=0.12\pm0.01$. The best fit from Eqs. (6) gives identical values of η with $D_a\simeq0.35\times10^{-7}$ cm^2/sec and $D_d\simeq0.7\times10^{-7}$ cm^2/sec. The best fit from Eq. (7) gives $D_a\tau_m\simeq1.0\times10^{-10}$ cm^2 and $D_d\tau_m\simeq2.1\times10^{-10}$ cm^2, which gives a value of $\tau_m\sim3$ msec for both cases and is in agreement with the observed length of the free-induction decay (where it decays into the noise). The approximation used in the simplification of Eqs. (6) to obtain Eq. (7) appears justified in these examples and all others we have tested.

It is seen from Fig. 2 that, except for the position of the singular peaks, we are not able to obtain a completely perfect fit using Eqs. (6) to the patterns, which is noticeable from the relative intensity of the central part of the spectrum, which is too high or too low. We are not sure of the reason for this. On the other hand, there is some fine structure which sometimes appears in the center of the experimental patterns which Eqs. (6) predicts. This is illustrated in Fig. 3, which shows both an experimental curve and that calculated from Eqs. (6). We have not been able to fit well the positions of the fine structure but only predict its presence. The fine structure depends on all the fitting-parameter values but it is particularly sensitive to the values of the line-broadening parameters W' and W''. Keeping constant the other variables, the fine structure becomes more evident when the singularities are more sharp. This behavior could be due to the fact that for longer free-induction decays the diffusion brings about larger molecular displacement during the time of measurement. This effect might become more pronounced for more sharp spectral lines. The spectral lines in the untwisted sample used here are broadened because

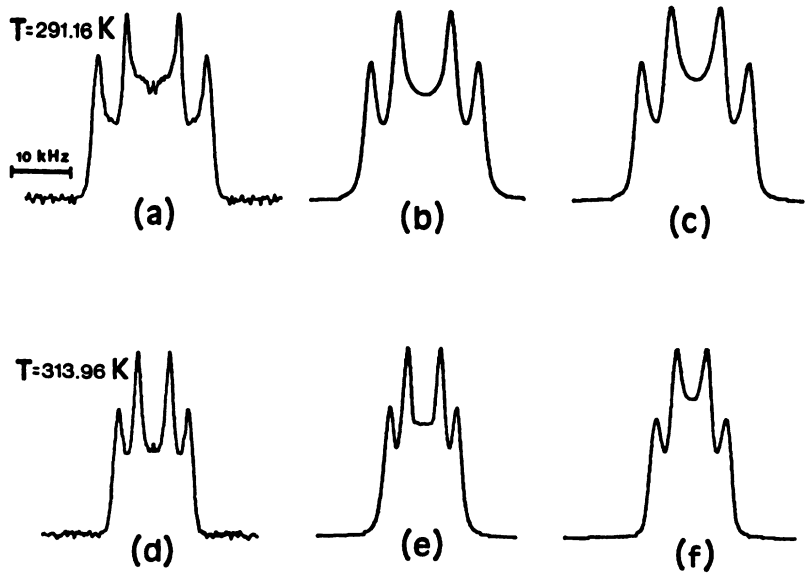

FIG. 2. Spectral patterns: experimental patterns (a) and (d); calculated patterns using Eqs. (6): (b) and (e); calculated patterns using Eqs. (7): (c) and (f), respectively. The best-fit parameters used in the calculated patterns are indicated in the text. Line-broadening parameters are $W'=1.3$ kHz and $W''=0.1$ kHz for both (b) and (c); $W'=1.2$ kHz and $W''=0.4$ kHz for both (e) and (f).

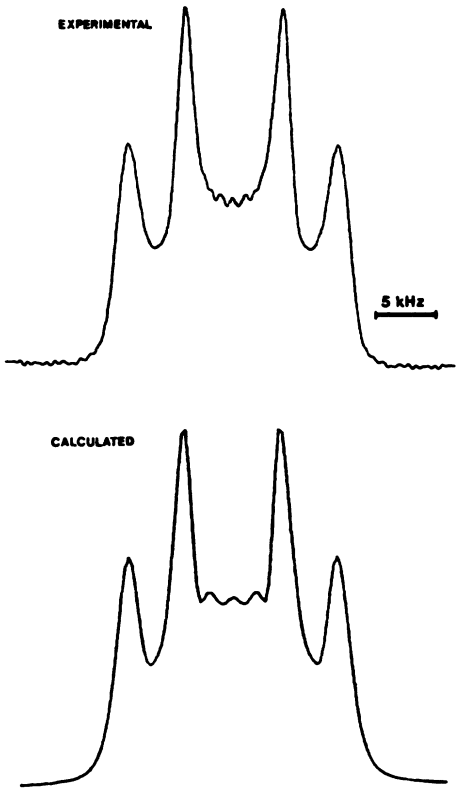

FIG. 3. Spectral patterns illustrating the fine structure which sometimes appears in the center of the pattern. The experimental pattern was obtained from a nematic mixture consisting of 58.6%, 40,7-d_4 and 41.4% MBBA to which was added 16.2% chiral MBMBA (Ref. 21) at the temperature 29.56°C. The calculated pattern using Eqs. (6) represents the best fit with the parameters $\eta=0.06$, $D=0.35\times10^{-7}$ cm^2/sec, $W'=1.35$ kHz, and $W'=0.75$ kHz.

of slightly inequivalent deuterium in the aromatic ring.

Another observation is that it is seen that Fig. 2(a) is better fit than Fig. 2(d). This observation could be due to fluctuations in the direction of the pitch axis that become more important as the temperature increases. Recently, Luz *et al.*[3] took into consideration these kinds of fluctuations.

III. DISTORTED HELICAL STRUCTURE

As is well known,[22] a cholesteric structure which aligns with the pitch perpendicular to $\vec{H}$ can be distorted by the magnetic field. The resulting powder pattern differs from that of the undistorted sample because of two effects: (i) The fraction of the molecules which align parallel to $\vec{H}$ increases with respect to those aligned perpendicular to $\vec{H}$. As a consequence, the relative intensities of the singularities are dramatically affected. (ii) It must be expected that for self-diffusion along the pitch axis, the averaging effect on the quadrupolar interaction should be different for each value of θ_0. The splitting corresponding to the zero-degree singularities should be less affected than the one corresponding to the inner singularities, since the interaction with the magnetic field reduces the twist angle in the region around $\theta_0=0$. The introduction of these effects in our diffusion model can be easily made by the equations of de Gennes,[22] which described the distorted structure. The variation of the angle θ, with respect to the change in coordinate x along the pitch axis, can be expressed as

$$\frac{dx}{d\theta}=\frac{p_0E(k)}{\pi^2}\left[\frac{1}{(1-k^2\cos^2\theta)^{1/2}}\right] \tag{9}$$

(the angle θ is equal to $\pi/2-\phi$, where ϕ is the angle used in the de Gennes' paper) in Eq. (9) $E(k)$ is the complete elliptic integral of second kind and k is a factor defined from the relation $k=E(k)H/H_c$, where H_c is the critical field for which the cholesteric is totally untwisted forming a nematic. Using Eq. (9) a new density probability function $P(\theta_0,\theta,t)$ and a new distribution function $U(\theta_0)$ can be obtained and used in Eq. (4) to obtain the averaged frequency of a distorted cholesteric:

$$\bar{\omega}(\theta_o,t)=\pm\tfrac{3}{16}\nu_Q\{[1-\eta]+[3+\eta]F(\theta_0,k,D,t)\}\ , \tag{10a}$$

with

$$F(\theta_0,k,D,t)=\frac{R(k)}{\sqrt{2\pi}\sigma}\int_{-\infty}^{+\infty}\frac{d\theta\cos2\theta}{\left[1-k^2\cos^2\theta\right]^{1/2}}\exp\left[-\frac{R(k)}{\sqrt{2}\sigma}\int_{\theta_0}^{\theta}\frac{d\alpha}{\left[1-k^2\cos^2\alpha\right]^{1/2}}\right]^2 \tag{10b}$$

and

$$R(k)=\frac{p_0E(k)}{\pi^2},\quad \sigma=\sqrt{2Dt}\ . \tag{10c}$$

The distribution function now becomes

$$U(\theta_0)=\frac{p_0E(k)}{\pi^2}\frac{1}{\left[1-k^2\cos^2\theta_0\right]^{1/2}}\ . \tag{11}$$

Equations (10) and (11) can be inserted in Eq. (5) in order to calculate the free-induction decay. A numerical calculation of Eq. (5) is very time consuming, since for each point of the free-induction decay it is necessary to calculate an integral over dt, $d\theta_0$, $d\theta$, and $d\alpha$, and use at least 1000 points in the time domain in order to obtain a spectrum in which the frequency domain is represented by a sufficient number of points. Therefore, we found it convenient to use Eq. (7) in which, as previously discussed, it is necessary to use the time of the measurement t_m. As in the case of the undistorted helix, the approximation used to obtain Eq. (7) should not significantly influence the shape of the spectrum. In Fig. 4 we show theoretical spectra obtained for different degrees of distortion as well as values of the diffusion constant. The spectra were obtained for $\eta=0$ and for a constant value of ν_Q and $p_0=3\mu$m. It is seen from Fig. 4 that, for a given distortion, the position of the inner singularity is most strongly affected by the larger the diffusion rate. On the other hand, for constant diffusion, our model predicts that when increasing the degree of distortion, both the intensity and the splitting of the inner singularities are strongly affected. Such spectra have not been observed experimentally, the reason being attributed to a possible new effect that has not been taken into account here. This effect is space modulation of the diffusion constant by the distorted helix. In the distorted structure there are periodic regions where there is no twist separated by regions of tight twist. Because of the apparent dependence of the diffusion constant on the value of the pitch,[5] the twisted regions act somewhat as barriers to diffusion, and the rate of diffusion is reduced in those regions to influence motional averaging and, consequently, the spectral shape. This effect is to be discussed elsewhere.[13]

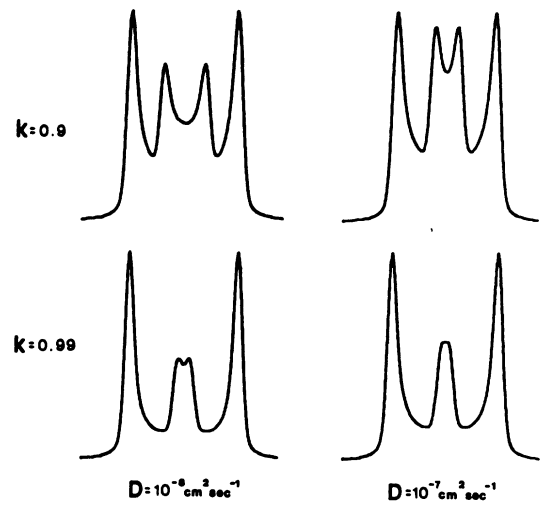

FIG. 4. Calculated spectral patterns for different degrees of distortion indicated by $k=0.9$ (weakly distorted) and $k=0.99$ (strongly distorted) and for different self-diffusion constants D. These spectral patterns were calculated assuming uniform diffusion rates along the pitch axis.

IV. CONCLUSION

In the case where the cholesteric helix is not distorted by the magnetic field we are able to obtain good fits to the experimental deuterium spectral patterns with two fitting parameters, the quadrupole asymmetry parameter η and the self-diffusion constant D. Because of the presence of edge singularities in the spectral patterns, we are able to measure small values of η with high precision, as well as obtain direct measurements of D from numerical fits to the patterns.

We find that the numerical fits can be greatly simplified with no apparent loss in the accuracy of the measurements of η if, instead of considering the quadrupole frequency to progressively change during the time of the measurement (free-induction decay), we consider an average quadrupole frequency which remains constant during the measurement. In this case, the fitting parameters become η and the product $D\tau_m$, where τ_m is the length of the free-induction decay. The latter fitting parameter is similar to that of Luz *et al.* who fit the product $D\nu_Q^{-1}$ but who used different calculational methods and did not include the parameter η. This could be why the values of the diffusion constant reported by Luz *et al.* are larger ($D \gtrsim 10^{-6}$ cm^2/sec) than those we report here $D \lesssim 10^{-7}$ cm^2/sec in that $\tau_m > \nu_Q^{-1}$. We have an additional check on our determined values of D, in that in our exact calculation we can fit D directly instead of the product of D and a characteristic time. Furthermore, our smaller values of D appear to be in better agreement with values measured by other techniques.[23]

In this paper we also show a simple expression whereby the values of η and $D\tau_m$ can be deter-

mined simply by the splittings between the edge singularities instead of the more complicated numerical fits.

In the case where the helix is distorted by the magnetic field, we find that the experimental spectral patterns cannot be fit if we consider the diffusion constant to be uniform along the pitch axis. We attribute this to a space modulation of the diffusion constant where periodic regions of tight twist modulate the diffusion constant. This feature is discussed in a subsequent paper.

ACKNOWLEDGMENTS

The authors are grateful to Prof. Kenneth Jeffrey and to Dr. Mark A. Rance, University of Guelph, Ontario, Canada for supplying us with computer programs helpful in calculating the fittings. We acknowledge the support by the National Science Foundation under Grant No. DMR 79-04393 and magnet facilities Grant No. DMR 78-09046. One of us (G. C.) is a recipient of a NATO Fellowship.

---

*On leave from Calabria University, Italy.
†On leave from the Centro de Fisica da Materia Condensada, Lisbon, Portugal.

[1]P. J. Collings, T. J. McKee, and J. R. McColl, J. Chem. Phys. 65, 3520 (1976).
[2]P. J. Collings and J. R. McColl, J. Chem. Phys. 69, 3371 (1978).
[3]Z. Luz, R. Poupko, and E. T. Samulski, J. Chem. Phys. 74, 5825 (1981).
[4]Z. Yaniv, N. A. P. Vaz, G. Chidichimo, and J. W. Doane, Phys. Rev. Lett. 47, 46 (1981).
[5]Z. Yaniv, G. Chidichimo, N. A. P. Vaz, and J. W. Doane, Phys. Lett. 86A, 297 (1981).
[6]C. E. Tarr, M. E. Field, L. R. Whalley, and K. R. Brownstein, Mol. Cryst. Liq. Cryst. 35, 231 (1976).
[7]G. R. Luckhurst and H. J. Smith, Mol. Cryst. Liq. Cryst. 20, 319 (1973).
[8]E. Sackmann, S. Meiboom, and L. C. Snyder, J. Am. Chem. Soc. 89, 5981 (1967).
[9]R. G. Priest and T. C. Lubensky, Phys. Rev. A 9, 893 (1974).
[10]A. Wulf, J. Chem. Phys. 59, 1497 (1973); 59, 6596 (1973).
[11]H. Schroeder, in *Liquid Crystals of One- and Two-Dimensional Order,* edited by W. Helfrich and G. Heppke (Springer, Amsterdam 1980), p. 196.
[12]W. Helfrich, Phys. Rev. Lett. 23, 372 (1969).
[13]N. A. P. Vaz, G. Chidichimo, Z. Yaniv, and J. W. Doane, Phys. Rev. A (unpublished).
[14]A. Abragam, *The Principles of Nuclear Magnetism* (Oxford University Press, London, 1961).
[15]N. A. P. Vaz and J. W. Doane, Mol. Cryst. Liq. Cryst. 68, 11 (1981).
[16]H. S. Gorslow and J. S. Jaeger, *Conduction of Heat in Solids* (Oxford University Press, London, 1959).
[17]J. H. Davis, K. R. Jeffrey, M. Bloom, M. I. Valic, and T. P. Higgs, Chem. Phys. Lett. 42, 390 (1976).
[18]D. J. Photinos, P. J. Bos, J. W. Doane, and M. E. Neubert, Phys. Rev. A 20, 2203 (1979).
[19]J. Pirs, P. Ukleja, and J. W. Doane, Solid State Commun. 19, 877 (1976).
[20]B. Melz, J. Charvolin, and P. Keller, Chem. Phys. Lipids 15, 161 (1975).
[21]D. Dolphin, Z. Muljiani, J. Cheng, and R. B. Meyer, J. Chem. Phys. 58, 413 (1973).
[22]P. G. de Gennes, Solid State Commun. 6, 163 (1968).
[23]H. Hakemi and M. M. Labes, J. Chem. Phys. 63, 3708 (1975).